Cardiovascular Research (2008) **77**, 766–773
doi:10.1093/cvr/cvm089

Dystrophic cardiomyopathy: amplification of cellular damage by Ca^{2+} signalling and reactive oxygen species-generating pathways

Carole Jung[1], Adriano S. Martins[2], Ernst Niggli[1], and Natalia Shirokova[2]*

[1]*Department of Physiology, University of Bern, Bern, Switzerland; and* [2]*Department of Pharmacology and Physiology, UMDNJ—New Jersey Medical School, 185 S. Orange Avenue, Newark, NJ 07103, USA*

Received 18 January 2007; revised 13 November 2007; accepted 22 November 2007; online publish-ahead-of-print 4 December 2007

Time for primary review: 34 days

KEYWORDS
Calcium (cellular);
Mitochondria;
Myocytes;
Oxygen radicals;
SR (function)

Aims Cardiac myopathies are the second leading cause of death in patients with Duchenne and Becker muscular dystrophy, the two most common and severe forms of a disabling striated muscle disease. Although the genetic defect has been identified as mutations of the dystrophin gene, very little is known about the molecular and cellular events leading to progressive cardiac muscle damage. Dystrophin is a protein linking the cytoskeleton to a complex of transmembrane proteins that interact with the extracellular matrix. The fragility of the cell membrane resulting from the lack of dystrophin is thought to cause an excessive susceptibility to mechanical stress. Here, we examined cellular mechanisms linking the initial membrane damage to the dysfunction of dystrophic heart.

Methods and results Cardiac ventricular myocytes were enzymatically isolated from 5- to 9-month-old dystrophic *mdx* and wild-type (WT) mice. Cells were exposed to mechanical stress, applied as osmotic shock. Stress-induced cytosolic and mitochondrial Ca^{2+} signals, production of reactive oxygen species (ROS), and mitochondrial membrane potential were monitored with confocal microscopy and fluorescent indicators. Pharmacological tools were used to scavenge ROS and to identify their possible sources. Osmotic shock triggered excessive cytosolic Ca^{2+} signals, often lasting for several minutes, in 82% of *mdx* cells. In contrast, only 47% of the WT cardiomyocytes responded with transient and moderate intracellular Ca^{2+} signals. On average, the reaction was 6-fold larger in *mdx* cells. Removal of extracellular Ca^{2+} abolished these responses, implicating Ca^{2+} influx as a trigger for abnormal Ca^{2+} signalling. Our further experiments revealed that osmotic stress in *mdx* cells produced an increase in ROS production and mitochondrial Ca^{2+} overload. The latter was followed by collapse of the mitochondrial membrane potential, an early sign of cell death.

Conclusion Overall, our findings reveal that excessive intracellular Ca^{2+} signals and ROS generation link the initial sarcolemmal injury to mitochondrial dysfunctions. The latter possibly contribute to the loss of functional cardiac myocytes and heart failure in dystrophy. Understanding the sequence of events of dystrophic cell damage and the deleterious amplification systems involved, including several positive feed-back loops, may allow for a rational development of novel therapeutic strategies.

1. Introduction

Dystrophinopathies result from mutations of the dystrophin gene (reviewed in Ervasti and Campbell[1]). Dystrophin is a 427 kDa protein linking the cytoskeleton to a complex of transmembrane proteins, which interact with the extracellular matrix. Duchenne and Becker muscular dystrophy (DMD and BMD) are the two most common and severe forms and are characterized by progressive and disabling muscle weakness (one case per 3500 boys). Cardiac manifestations are present in essentially all patients by 20 years of age. The most common abnormality is dilated cardiomyopathy. Around 20% of the patients succumb from the cardiac manifestations. Clinically, the disease initially shows ECG abnormalities. Later, echocardiographic examinations reveal ventricular wall motion abnormalities in regions of fibrosis. With spreading of fibrosis, ventricular dysfunction and arrhythmias occur, ultimately leading to heart failure and sudden death.[2] With improving medical care for the skeletal muscle weakness, the cardiac disease becomes more and more limiting for the survival of the patients.

In the skeletal muscle field, there is a significant body of data describing the cellular pathophysiological events (for review see Allen *et al.*[3]). It is generally believed that the

* Corresponding author. Tel: +1 973 972 8877; fax: +1 973 972 7950.
E-mail address: nshiroko@umdnj.edu

dystrophin deficiency leads to exaggerated sarcolemmal fragility. Abnormal Ca^{2+} influx and intracellular Ca^{2+} homeostasis after mechanical stress have been implicated in progressive death of dystrophic skeletal muscle fibres.[4,5] The *mdx* mouse is a well-established model for skeletal muscle dystrophy, and it also develops a cardiac phenotype with age that is similar to the alterations observed in humans during dystrophic cardiomyopathy.[6] It is suggested that in skeletal muscle Ca^{2+} entry could occur *via* voltage-independent pathways,[3] such as 'leak' channels,[7] stretch-activated channels (SAC),[8] or store operated channels (SOC).[9] The molecular identity of these channels is not yet fully clear, but some of them are thought to contain TRP channel subunits.[3] In addition, there are findings suggesting that the vulnerability of *mdx* muscle leads to microruptures which may also allow excessive Ca^{2+} influx.[10] Despite all these identified possible pathways for Ca^{2+} entry, the main question still remains open: what is the sequence of cellular events that initiate Ca^{2+} influx and which are the positive feed-back loops that amplify this influx and lead to Ca^{2+} overload and cell death?

Identical questions apply to the cardiac phenotype, but much fewer studies were carried out to understand cellular mechanisms leading to cardiac pathology. However, the clinical findings described above and some experimental studies on the organ level also indicate an abnormal sensitivity of cardiomyocytes to mechanical stress, for example, after aortic banding[11] or prolonged exposure to β-adrenergic stimulation to induce arterial hypertension.[12] In addition, histological examination revealed replacement of muscle with connective tissue and the presence of apoptotic and necrotic myocytes, also in cardiac muscle.[13,14] Thus, cell death most likely underlies the development of fibrosis and progressive deterioration of both tissues.

A functional study found a high stress sensitivity of isolated *mdx* cardiomyocytes and that the cell damage could be suppressed by the membrane protective detergent Poloxamer P188.[15] In addition, a report suggested SAC to contribute to the abnormal Ca^{2+} influx pathway in *mdx* myocytes.[16] Here, we used confocal imaging with various fluorescent indicators to monitor intracellular processes that may link the initial transmembrane Ca^{2+} influx to cell damage. We observed that *mdx* cardiac myocytes exhibit an extreme Ca^{2+} signalling response to mechanical stress. More importantly, we identified an abnormal activation of the Ca^{2+}-induced Ca^{2+} release signalling pathway together with an increased generation of reactive oxygen species (ROS) as two synergistic mechanisms contributing to the amplification of these Ca^{2+} signals. Preliminary results of these studies have been published as an abstract.[17]

2. Methods

2.1 Cell isolation

Ventricular myocytes were enzymatically isolated from 5- to 9-month-old mice as previously described.[18,19] The study conforms with the *Guide for the Care and Use of Laboratory Animals* published by the US National Institutes of Health (NIH Publication No. 85-23, revised 1996). C57BL/10ScSn-*mdx* and wild-type (WT) mice with identical genetic background (5–10 months old) were provided by Drs M. Rüegg (University of Basel, Switzerland), U. Rüegg (University of Geneva, Switzerland), or purchased from the Jackson laboratory (USA).

2.2 Experimental solutions

The isotonic superfusion solution contained (in mM): 140 NaCl, 5.4 KCl, 1.8 $CaCl_2$, 1.1 $MgCl_2$, 5 HEPES, and 10 glucose. The osmolality was ∼310 mosm/kg, and pH 7.3. The hypotonic solution contained 70 mM NaCl instead of 140 mM, had osmolality ∼170 mosm. Zero Ca^{2+} solution contained 2 mM EGTA. Where indicated, apocynin or ryanodine and thapsigargin were added for at least 30 min before the experiment. Most chemicals were obtained from Sigma. Mn-cpx 3 and apocynin were from Calbiochem, ryanodine from Alamone. All experiments were performed at room temperature (20–22°C).

2.3 Confocal microscopy

Changes in cytosolic and mitochondrial [Ca^{2+}], ROS production, and mitochondrial membrane potential were monitored with fluorescent indicators fluo-3 AM (5 μM), rhod-2 AM (5 μM), fura-red AM (5 μM), 5-(and-6)-chloromethyl-2′,7′-dichlorodihydrofluorescein diacetate (CM-H_2DCFDA; 20 μM), and tetramethylrhodamine ethyl ester (TMRE; 100 nM), as previously described.[20–22] As a rule, cells were incubated with indicators for 30 min at room temperature, followed by at least 15 min for de-esterification. Resting [Ca^{2+}] and Ca^{2+} influx were measured with a double-indicator ratiometric procedure, which simultaneously utilizes fluo-3 and fura-red indicators to correct for dye dilution during osmotic swelling.[23] Fluo-3 AM was from Biotium, other indicators were from Invitrogen. A laser-scanning confocal microscope (Radiance, Bio-Rad) was used to acquire confocal images.[22,24] Fluo-3, fura-red, and CM-H_2DCFDA were excited with the 488 nm line of an Argon laser. TMRE and rhod-2 were excited with a HeNe laser at 543 nm. The emitted light was collected above 500 nm and above 570 nm, respectively. The emission of fluo-3 and fura-red was simultaneously recorded with two PMTs using 515/30 and >600 nm emission filters and the ratio calibrated according to.[23]

2.4 Data analysis

Analysed data are represented as mean ± SEM. Where stated, statistical significance was determined using Student's *t*-test or the log-rank test. In the figures, single asterisk indicates $P < 0.05$, double asterisks indicate $P < 0.01$.

3. Results

3.1 Osmotic shock triggers excessive cytosolic Ca^{2+} signals in *mdx* but not wild-type cardiomyocytes

We applied osmotic shocks to mimic some of the pathophysiological conditions of mechanical stress encountered by the cell *in vivo*.[5,25] Hypotonic solution induces cell swelling and mechanical deformation of the cell membrane. Cytosolic Ca^{2+} transients were recorded in both WT and *mdx* cardiomyocytes loaded with fluo-3. As a rule, series of 100 *XY* confocal scans were acquired at 0.5 Hz. Exposure of the cardiac myocytes to hypotonic solution (170 mosm) for 40 s consistently resulted in reversible cell swelling (by 15.8 ± 1.5%, $n = 34$). In 82% of *mdx* myocytes (19 out of 23 cells), the return to isotonic solution caused extreme cytosolic Ca^{2+} signals such as bursts of Ca^{2+} sparks and repetitive Ca^{2+} waves exhibiting amplitudes comparable with normal Ca^{2+} transients (as shown in *Figure 1A*, left panel). In the majority of *mdx* cells, these Ca^{2+} signals lasted for the full duration of the recording (up to 3 min). In contrast, in only 47% of the WT cardiomyocytes, osmotic shock produced Ca^{2+} signals (nine out of 19 cells) and these were mostly moderate and short-lived (*Figure 1A*, right panel). The typical Ca^{2+} responses in *mdx* and WT

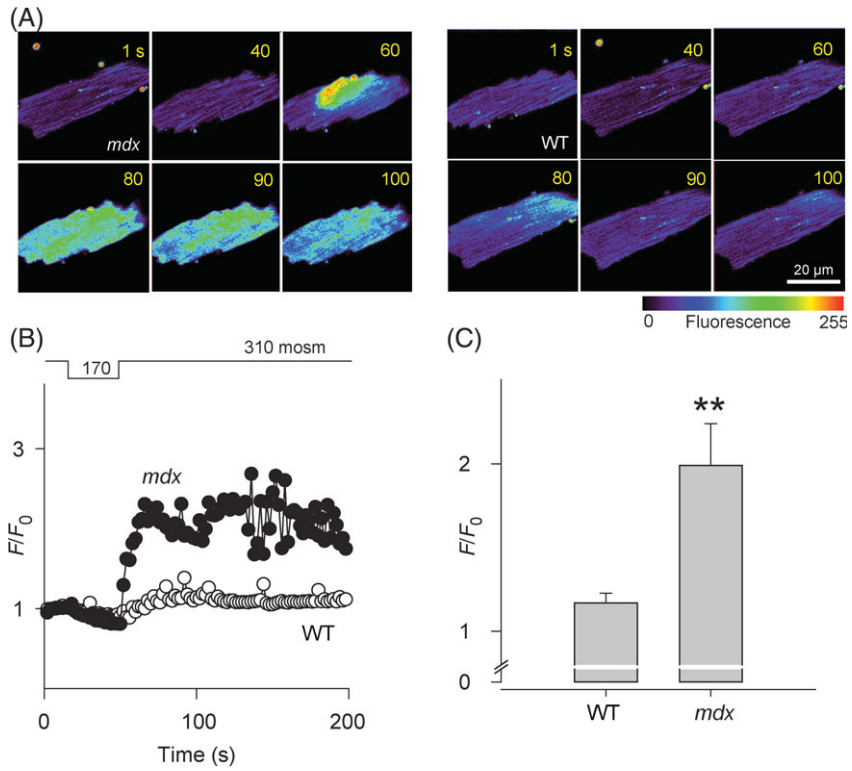

Figure 1 Stress-induced intracellular Ca^{2+} signals in *mdx* and wild-type (WT) mouse ventricular myocytes. (*A*) Images of Ca^{2+}-related fluorescence (fluo-3) obtained in *mdx* (left) and WT (right) myocytes subjected to osmotic shock. Ca^{2+} sparks and Ca^{2+} waves appear after the shock, much more pronounced in the *mdx* myocyte (left panel). (*B*) Time course of normalized fluorescence pooled from this protocol in *mdx* (black circles) and WT myocytes (white circles). Line on the top represents the protocol by which extracellular solutions were changed. (*C*) Mean values of normalized fluorescence averaged for each cell during 60 s after the osmotic shock (for *B* and *C*: $n = 23$ cells from $N = 4$ mice for *mdx* and $n = 19$, $N = 3$ for WT).

cells are also visualized in movies in the online supplement. *Figure 1B* shows the averaged changes in intracellular fluorescence in all studied WT and *mdx* cardiomyocytes, normalized to the resting values before osmotic shock. The stress-induced increase in fluorescence was larger and longer lasting in *mdx* cells compared with WT myocytes. The mean cellular fluorescence signal recorded during the first 60 s after returning to the iso-osmotic solution was 6-fold larger in *mdx* cells (*Figure 1C*).

3.2 A small Ca^{2+} influx is required for stress-induced Ca^{2+} signals in *mdx* cardiomyocytes

The above observation together with the recent results by Yasuda *et al.*[15] suggest that *mdx* myocytes are more susceptible to membrane damage than WT cardiomyocytes. To test whether these Ca^{2+} signals depend on extracellular Ca^{2+}, we briefly removed Ca^{2+} from the extracellular solution. *Figure 2* shows that switching to a solution containing 0 mM Ca^{2+} completely abolished the response to osmotic shock. This observation confirms that Ca^{2+} entry is required, although the precise pathway(s) leading to Ca^{2+} influx into dystrophic cells are yet to be established and seems to involve multiple molecular entities.[3]

Nevertheless, the increase in plasmalemmal permeability to Ca^{2+} and the slightly elevated resting Ca^{2+} concentration in *mdx* myocytes (see *Figure 2E* and Williams and Allen[16]) alone are unlikely to explain the sustained Ca^{2+} signals in *mdx* cells subjected to osmotic shock. In cells treated with ryanodine (5 µM) and thapsigargin (500 nM) to eliminate the function of the sarcoplasmic reticulum (SR), a substantial Ca^{2+} influx during the superfusion with hypotonic solution would be visible as an increase of the cytosolic Ca^{2+} concentration. However, when applying a ratiometric indicator technique involving fluo-3 and fura-red to compensate for dye dilution due to osmotic swelling, only a modest elevation of the Ca^{2+} concentration was observed, suggesting that the Ca^{2+} influx was small (*Figure 2C* and D, gray circles).

3.3 Osmotic shock stimulates reactive oxygen species production

Because we were not able to detect a substantial Ca^{2+} influx during the shock, we suspected some intracellular mechanisms by which even small increases in $[Ca^{2+}]_i$ due to Ca^{2+} influx were amplified. One possibility could be oxidation of the cytosolic environment due to excessive ROS production,[26] which could affect several proteins involved in intracellular Ca^{2+} homeostasis, most notably the ryanodine receptors (RyRs), thereby enhancing the sensitivity of SR Ca^{2+} release.

To test whether osmotic shock enhances ROS generation, we loaded myocytes with CM-H_2DCFDA. In cells, this nonfluorescent compound is hydrolysed to DCFH and ROS generation is detected as a result of DCFH oxidation to DCF. *Figure 3A* shows images from one *mdx* cardiac myocyte before (image at 20 s), during (50 s), and after osmotic shock (80, 110, 140, and 170 s). Insets illustrate the banded fluorescence typical of a mitochondrial distribution. *Figure 3B* represents averaged and normalized

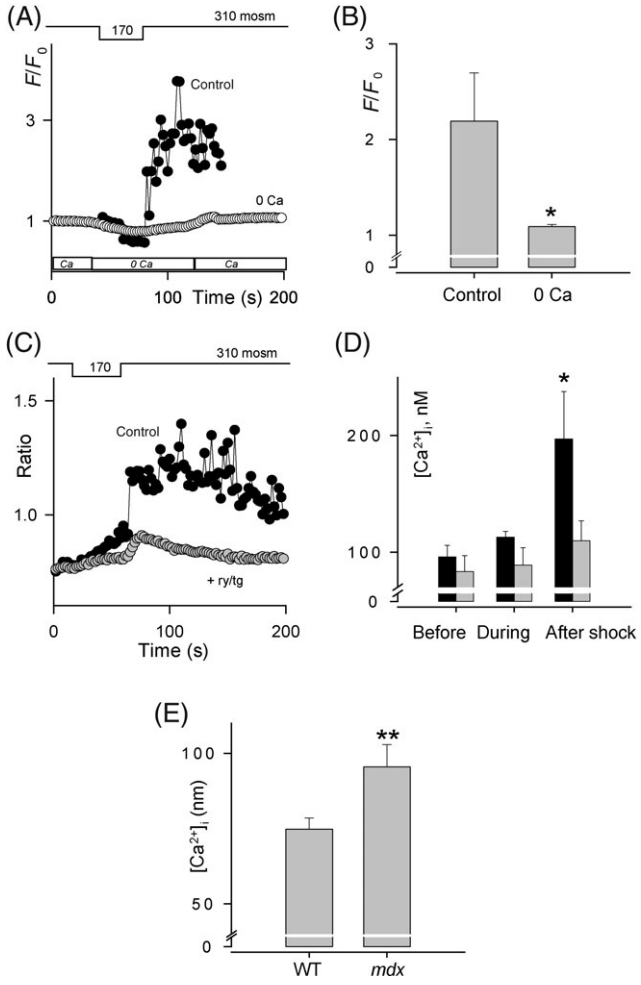

Figure 2 Removal of extracellular Ca^{2+} prevents stress-induced Ca^{2+} signals while Ca^{2+} influx during osmotic shock is small. (*A*) Time course of averaged normalized fluorescence in *mdx* cells during the osmotic shock under control conditions (black circles) and when Ca^{2+} was briefly removed from the external solution (white circles). Bars at the bottom illustrate protocol by which extracellular solutions were changed. (*B*) Mean averaged fluorescence after the osmotic shock in the presence and absence of extracellular Ca^{2+} (for *A* and *B*: $n = 5$ cells from $N = 2$ mice for control and $n = 6$, $N = 2$ for zero Ca^{2+}). (*C*) Time course of averaged fluo-3/fura red ratio in *mdx* myocytes in control (black circles) and in the presence of ryanodine (ry, 5 μM) and thapsigargin (tg, 0.5 μM) (gray circles). (*D*) Mean $[Ca^{2+}]$ before, during, and 60 s after the osmotic shock in control ($n = 7$, $N = 3$) and in the presence of ryanodine and thapsigargin ($n = 8$, $N = 3$). (*E*) Mean resting $[Ca^{2+}]$ in wild-type and *mdx* cardiomyocytes ($n = 70$ and 59, $N = 4$ and 4 mice).

changes in DCF fluorescence in *mdx* and WT cells. To quantify the stress-induced changes in ROS production, we performed a linear fit to the fluorescence signal in each cell before and after osmotic shock. The slope of the DCF signal reflects the rate of ROS production. Before the osmotic shock, the ROS-related signals rose monotonically, presumably due to a basal generation of ROS. The initial slope was significantly larger in *mdx* myocytes than in WT cells (0.70 ± 0.09, $n = 12$ and 0.40 ± 0.07, $n = 9$, respectively) indicating an oxidative stress in these cells, as also suggested in Williams and Allen.[27] Furthermore, we observed that the slope increased after the shock in both WT and *mdx* cells, but more in *mdx* myocytes than in WT cells [ratio of slopes before to after the shock was 1.72 ± 0.2 ($n = 12$) and 1.34 ± 0.12 ($n = 9$) in *mdx* and WT, respectively].

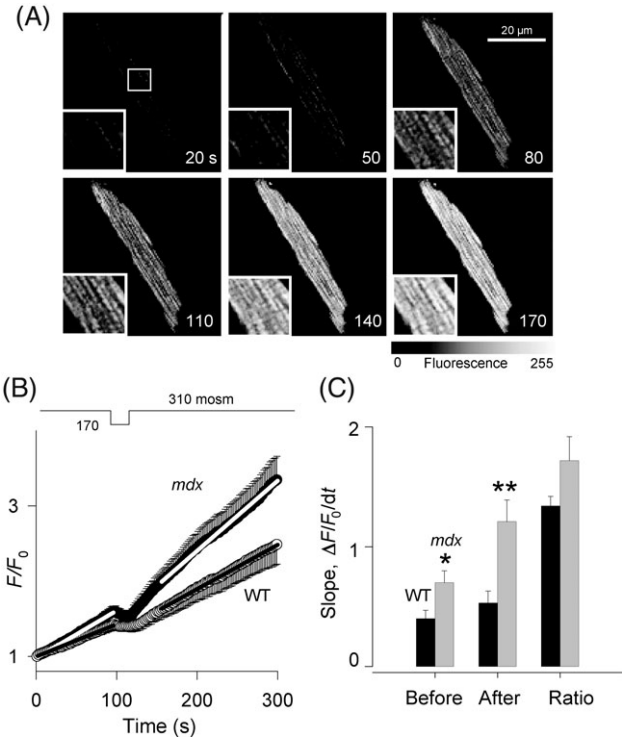

Figure 3 *Mdx* cells generate more ROS than wild type and react more pronounced to osmotic shock. (*A*) Images of ROS related fluorescence ($CM\text{-}H_2$-DCFDA) in *mdx* myocytes exposed to osmotic shock (insets show magnified region of interest indicated in first panel). (*B*) Averaged changes in normalized ROS signal in *mdx* (black circles) and wild-type (WT) (white circles) cells. Lines represent linear fits to the data. (*C*) *Mdx* myocytes generate more background ROS and after the stress their production of ROS increases more than in WT cells ($n = 12$ and 9, $N = 3$ and 3 mice). See Supplementary Material online for colour version.

To confirm the involvement of ROS-dependent mechanisms in the generation of stress-induced Ca^{2+} signals, we incubated *mdx* myocytes with 10 μM Mn-cpx3, a superoxide dismutase mimetic. *Figure 4A* shows that this ROS scavenger nearly eliminated cytosolic Ca^{2+} transients produced by osmotic shock. After washing out the scavenger for 30 min, five out of six *mdx* cardiomyocytes recovered their exacerbated response. *Figure 4B* shows a significant decrease in the mean intracellular fluorescence recorded during the first 60 s after returning to an iso-osmotic solution in the presence of the scavenger.

There are several possible sources of ROS in cardiac myocytes that may be activated in response to mechanical stress. NAD(P)H oxidase (NOX) is known to be overexpressed in dystrophic heart[27] and was found to be rapidly activated by osmotic swelling in astrocytes.[28] Therefore, we tested whether NOX could be a source for a rapid increase in the ROS production in response to the mechanical stress in *mdx* myocytes. Cells were incubated for 30 min with the NOX inhibitor apocynin (0.2–1 mM). *Figure 4C* and D shows that the drug nearly eliminated the intracellular Ca^{2+} signals induced by osmotic shock, suggesting NOX as a possible source of acute ROS production.

3.4 Excessive cytosolic Ca^{2+} is taken up by the mitochondria

Mitochondria are well-established sources of ROS in myocardium subjected to acute or chronic mechanical stress.[29]

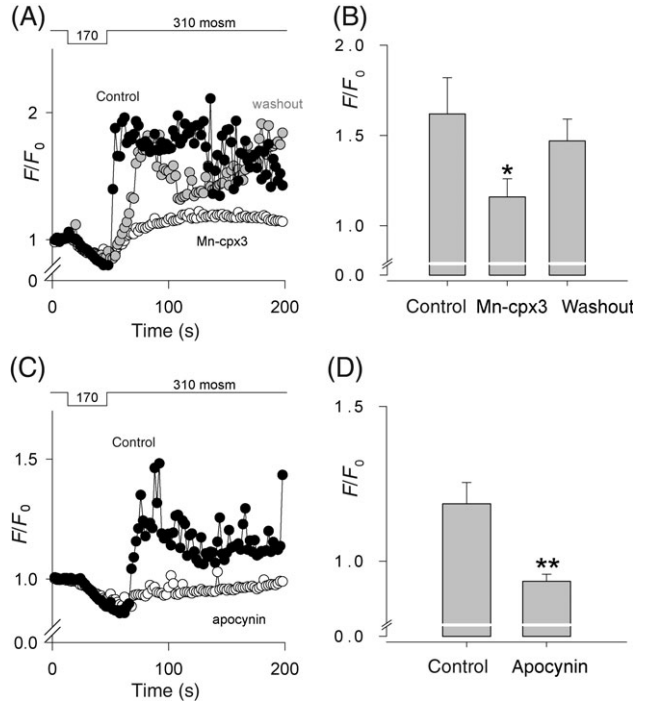

Figure 4 Stress-induced Ca^{2+} signals depend on reactive oxygen species (ROS). (*A*) Time course of averaged normalized fluo-3 fluorescence in *mdx* cells subjected to osmotic shock under control conditions (black circles), after incubation with 10 μM of the ROS scavenger Mn-cpx3 (white circles), and 30 min after its washout (gray circles). (*B*) Mean normalized fluorescence for data averaged during 60 s after the osmotic shock for control, Mc-cpx3, and after 30 min washout. Data for *A* and *B* are from $n = 6$, 6, and 11 cells, $N = 3$, 3 and 3 animals, respectively. (*C* and *D*) Time course and averages showing suppression of the Ca^{2+} responses by the NOX inhibitor apocynin (data from $n = 16$ and 27 cells, $N = 4$ and 4 mice).

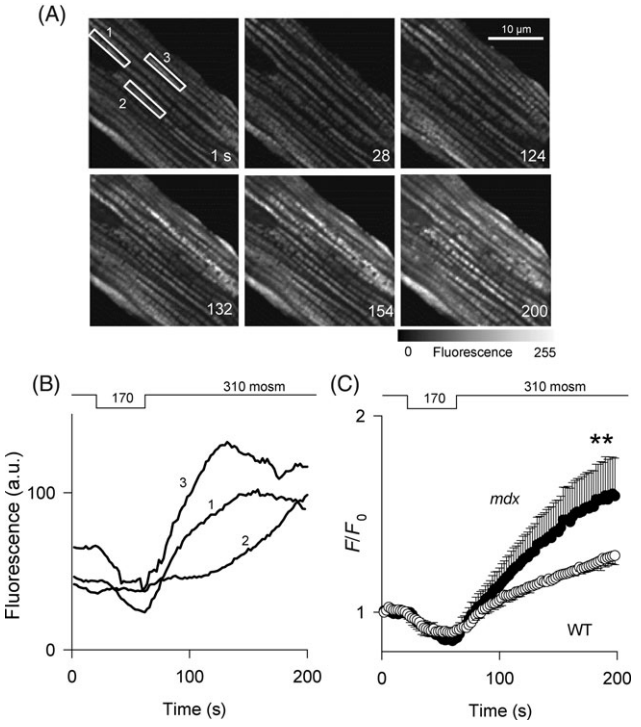

Figure 5 Excessive cytosolic Ca^{2+} is taken up by mitochondria. (*A*) Images of rhod-2 fluorescence in *mdx* myocyte undergoing osmotic shock. (*B*) Time course of rhod-2 signal in the groups of mitochondria indicated by regions of interest (1–3 in *A*). (*C*) Pooled data from *mdx* (black circles) and wild-type (white circles) cells studied with the same protocol. At the end of the recording, the mitochondrial Ca^{2+} accumulation is significantly more pronounced in *mdx* myocytes (data from $n = 6$ and 8 cells, $N = 2$ and 3 mice). See Supplementary Material online for colour version.

Mitochondrial ROS could be responsible for the sustained cellular Ca^{2+} signals observed in *mdx* myocytes (note the gradual increase in ROS-related fluorescence in the mitochondrial regions later during the experiment shown in *Figure 3*). It is known that muscle cells continuously generate ROS, as a by-product of the mitochondrial respiratory chain, and that enhanced mitochondrial Ca^{2+} uptake stimulates further mitochondrial ROS production. We tested whether and to what extent mitochondria take up cytosolic Ca^{2+} after osmotic shock.

Mdx and WT myocytes were loaded with the Ca^{2+} indicator rhod-2 and imaged with the identical experimental protocol. Rhod-2 is a charged molecule that preferentially partitions into the mitochondria. *Figure 5A* shows the mitochondrial rhod-2 distribution and the fluorescence signal in *mdx* myocytes before (image at 1 s), during (image at 28 s), and after the shock. Following 40 s of osmotic shock, fluorescence gradually increased within all mitochondria. *Figure 5B* shows the time course of rhod-2 signals in three groups of mitochondria indicated in *A*. In some mitochondria, the rhod-2 signal, after an initial rise, decreased at later times, indicating a loss of rhod-2 and Ca^{2+}. *Figure 5C* represents averaged normalized changes in rhod-2 fluorescence in six *mdx* and eight WT cells, indicating that following osmotic stress mitochondria in *mdx* myocytes sequester significantly more Ca^{2+} which can add to the more pronounced ROS production.

3.5 Osmotic shock induces mitochondrial depolarization in *mdx* cardiac myocytes

It is established that mitochondrial Ca^{2+} overload and the subsequent oxidative stress can lead to collapse of the mitochondrial membrane potential ($\Delta\psi_m$) and/or to the opening of the mitochondrial permeability transition pore (mPTP), ultimately causing necrotic/apoptotic cell death.[29] Our results indicate that mitochondrial Ca^{2+} uptake is enhanced in *mdx* cardiac myocytes. We also found that some mitochondria lose Ca^{2+} after a period of initial accumulation, possibly as a result of irreversible mitochondrial depolarization.[30] Therefore, we carried out experiments to directly monitor changes in mitochondrial membrane potential. TMRE is a charged dye, which distributes across the mitochondrial membrane in a voltage-dependent manner. Whenever the potential across the mitochondrial membrane dissipates, TMRE fluorescence is lost. *Figure 6A* shows one *mdx* cardiomocyte loaded with 100 nM TMRE. A single mitochondrion (or a small group of mitochondria) can be visualized in each of the marked boxes. Subsequent to the osmotic shock, some mitochondria displayed irreversible loss of $\Delta\psi_m$ whereas others did not. Changes in TMRE fluorescence for four individual mitochondria are plotted in *Figure 6B*. Note that the final level of TMRE signal is essentially the same in all four organelles, indicating their complete depolarization. *Figure 6C* compares the incidence and timing of osmotic shock-induced mitochondrial depolarization in *mdx* and WT cardiomyocytes. For each time point, we

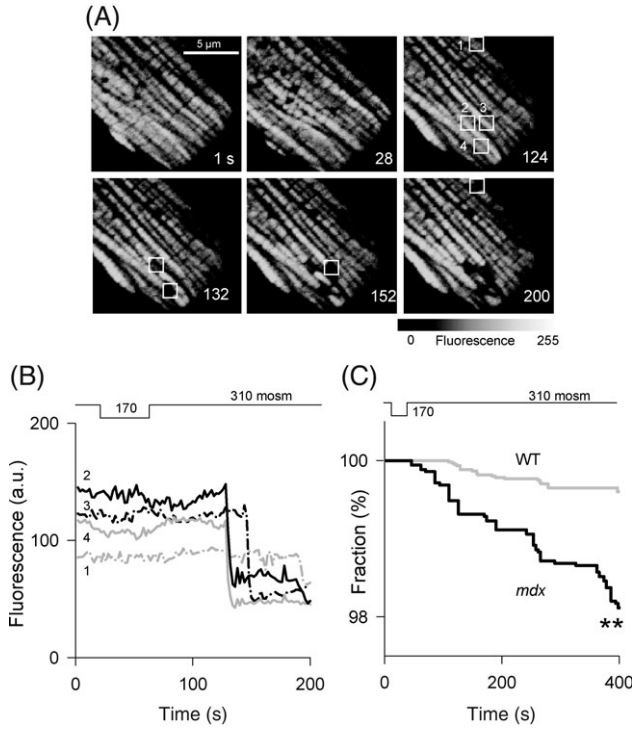

Figure 6 Stress-induced collapse of mitochondrial membrane potential. (*A*) Images of TMRE fluorescence in an *mdx* myocyte subjected to osmotic shock. (*B*) Stepwise changes in fluorescence in boxed mitochondria in *A* suggest sudden loss of the membrane potential. (*C*) Fraction of mitochondria remaining polarized after osmotic shock in *mdx* (black line) and wild-type (gray line) myocytes. In *mdx* myocytes, significantly larger fraction of mitochondria loose their potential within the recording time (data from $n = 10$ and 9 cells, $N = 3$ and 3 mice). See Supplementary Material online for colour version.

calculated the number of polarized mitochondria in all cells of each type and normalized it to the total numbers of organelles imaged. In *mdx* cells, osmotic shock induced depolarization of ~2% of the mitochondria within 400 s of experimental recording (black line). Loss of TMRE signals by individual mitochondria was observed already 4 s after the shock. In contrast, in WT myocytes, the fraction of depolarized mitochondria was much smaller (0.3%) and the onset was later (100 s after the shock). It should be mentioned that in some *mdx* myocytes shock induced severe mitochondrial depolarization waves that resulted in complete collapse of $\Delta\psi_m$ across the entire cell within a few seconds. These cells were not included in the analysis presented in *Figure 6C*.

4. Discussion

Dystrophin-deficient cardiomyocytes are vulnerable to mechanical stress. Recently published work connects increased membrane fragility and stretch-induced Ca^{2+} influx with death of dystrophic cells.[15] In the present study, we identified two cellular signal amplification mechanisms that may link the fragility of the *mdx* cardiomyocyte membrane to later cell damage. As detailed below, the simultaneous activation of these two signal amplification systems is detrimental, because of bidirectional cross-talk with positive feed-back. Thus, the cellular response proceeds beyond the physiological limits, culminating in a chain of events, which may later end in apoptotic and/or necrotic cell death.

4.1 Amplification mechanisms

The massive Ca^{2+} signals observed in *mdx* myocytes after osmotic shock were manifest as a surge of abundant spontaneous Ca^{2+} sparks, regularly blending into Ca^{2+} waves travelling along the cell. In resting cardiomyocytes such signals are the hallmark of abnormal Ca^{2+}-induced Ca^{2+} release (CICR) activation and are commonly initiated by overloading the SR with Ca^{2+} in the course of various noxious conditions. The importance of CICR for the observed signal amplification was also emphasized by the absence of such Ca^{2+} signals in cells pretreated with ryanodine and thapsigargin. However, for Ca^{2+} overload to develop in a short period of time (i.e. during the exposure to hypotonic solution), Ca^{2+} influx has to be substantial. Surprisingly, such a massive Ca^{2+} influx could not be detected in our experiments, even though the behaviour of the myocytes in zero Ca^{2+} indicated an important role for at least some minor transsarcolemmal Ca^{2+} influx. The obvious discrepancy between massive and rapid CICR activation despite minimal Ca^{2+} entry and only slightly elevated resting Ca^{2+} levels led us to consider additional mechanisms that could make the RyRs rapidly more sensitive and provoke spontaneous Ca^{2+} signals without pronounced SR Ca^{2+} overload.

ROS have been implied in changing gating and Ca^{2+} sensitivity of the RyRs via redox modifications of the channels.[31] Furthermore, increased ROS generation after mechanical stretch has been reported even in normal cardiac muscle.[26] Our findings revealed an elevated basal rate of ROS production in *mdx* cells. Furthermore, mechanical stress led to enhanced ROS production in all cardiomyocytes, but significantly more pronounced in *mdx* cells. Although the first finding may underlie the propensity of *mdx* cells to overreact after small Ca^{2+} influx signals, the latter may be a consequence of the larger Ca^{2+} signals in these cells. As one might expect based on these findings, ROS scavengers reversibly suppressed the excessive stress-induced Ca^{2+} signalling in *mdx* cells. Taken together, our results suggest that the change of the cytosolic oxidative environment due to increased [ROS] promotes the abnormal CICR activation without pronounced Ca^{2+} overload.

ROS generation in response to mechanical forces may originate from several sources, including the NOX, xanthine oxidase, or other oxidase systems, such as nitric oxide oxidase, and mitochondria. Our results with the NOX inhibitor apocynin suggest an involvement of this source of ROS. Owing to its overexpression in dystrophic heart[27] and due to its rapid activation by osmotic swelling,[28] this source of ROS may be particularly important in the early phases of the response. It is also established that an elevation in mitochondrial [Ca^{2+}] subsequent to prolonged cytosolic Ca^{2+} signal activity stimulates mitochondrial ROS production.[29] Consistent with this notion, we observed increased Ca^{2+} levels in cardiac mitochondria following the osmotic shock that were significantly larger in *mdx* cells.

4.2 Cross-talk between Ca^{2+}-induced Ca^{2+} release and reactive oxygen species

CICR and ROS generation are two signalling pathways that exhibit a high degree of positive feed-back. Either mechanism could lead to the observed massive Ca^{2+} signals. However, the combination of both pathways being activated together may have even more severe consequences, as both pathways exhibit mutual and synergistic cross-talk with each other. For example, ROS could promote RyRs openings as well as further increase membrane fragility due to lipid peroxidation. In addition, ROS could stimulate Ca^{2+} influx into the cells via SAC and/or SOC, as some TRP channels (potential candidates for SOC and SAC) have been shown to be sensitive to the redox potential of the cytosol.[3] On the other hand, CICR and elevated $[Ca^{2+}]_i$ favour mitochondrial ROS production, as discussed above. Taken together, the simultaneous activation of these signalling pathways is particularly destructive for the cells because it has a tendency to escalate into mutually synergistic positive feed-back signalling loops.

4.3 Link between abnormal cellular signalling and pathology of the heart

Although WT myocytes survive the initial Ca^{2+} overload, the strong activation of several pathways may overwhelm the cellular defence mechanisms in *mdx* cells. It has been postulated for many years that proteases are a downstream Ca^{2+}-activated target involved in protein degradation and necrosis of dystrophic skeletal muscle.[3] Calpain is considered to be a likely candidate, as its expression is greater in *mdx* muscle.[3] Because calpain is expressed in heart, and because calpain inhibitors protect from ischaemia–reperfusion injury,[32] it is likely that this protease forms a part of the cellular death pathway in *mdx* heart.

Under pathological conditions, cytosolic and mitochondrial Ca^{2+} overload and/or excess in ROS can lead to opening of the mPTP, which is accompanied by a dissipation of the mitochondrial membrane potential and usually precedes necrotic/apoptotic cell death.[29,33] Our data reveal multiple mitochondrial dysfunctions in *mdx* cardiac myocytes following osmotic stress. In particular, they show mitochondrial Ca^{2+} overload, increased ROS production, irreversible depolarization of the mitochondrial membrane, which can be a direct indication of mPTP opening. Apoptotic and necrotic cells have been observed in cardiac tissue of dystrophy patients and *mdx* mice. Lost cardiomyocytes cannot regenerate and are likely to be replaced by connective tissue, ultimately leading to the observed fibrosis.[2]

At present, several studies are conducted to develop treatments of the cardiac dystrophic phenotype by either replacing the lost cardiomyocytes with stem cell approaches[34] or to make the myocytes mechanically less vulnerable by gene transfer of dystrophin, utrophin, or functional dystrophin fragments (microdystrophins).[35] Notably, *mdx* mice can partly compensate for the lack of dystrophin by adaptive upregulation and redistribution of the protein utrophin.[36] An *mdx* mouse lacking utrophin presents with a more severe phenotype,[37] particularly in skeletal muscle, but also in cardiac muscle.[38] Although cell replacement therapies will obviously only be able to treat late stages of the disease, curative gene therapy may require a long time to develop for routine application. In the meantime, it would be helpful to implement pharmacological treatment options which are able to slow down the progression of the disease.[4] Considering the early cellular stress responses reported here, this might be accomplished by interfering with any of the early cellular events leading to excessive Ca^{2+} and ROS signals.

Supplementary material

Supplementary material is available at *Cardiovascular Research* online.

Acknowledgements

We thank Drs Mohammed Fanchaouy, Larry Gaspers, Jakob Ogrodnik, Roman Shirokov, and Andrew Thomas for discussions and Daniel Lüthi for technical assistance.

Funding

Swiss Foundation for Research on Muscle Diseases; Muscular Dystrophy Association; Swiss National Science Foundation; Swiss State Secretariat for Education and Research; UMDNJ & Sigrist Foundations.

Conflict of interest: none declared.

References

1. Ervasti JM, Campbell KP. Dystrophin-associated glycoproteins: their possible roles in the pathogenesis of Duchenne muscular dystrophy. *Mol Cell Biol Hum Dis Ser* 1993;**3**:139–166.
2. Finsterer J, Stollberger C. The heart in human dystrophinopathies. *Cardiology* 2003;**99**:1–19.
3. Allen DG, Whitehead NP, Yeung EW. Mechanisms of stretch-induced muscle damage in normal and dystrophic muscle: role of ionic changes. *J Physiol* 2005;**567**:723–735.
4. Rüegg UT, Nicolas-Metral V, Challet C, Bernard-Helary K, Dorchies OM, Wagner S *et al*. Pharmacological control of cellular calcium handling in dystrophic skeletal muscle. *Neuromuscul Disord* 2002;**12**:S155–S161.
5. Wang X, Weisleder N, Collet C, Zhou J, Chu Y, Hirata Y *et al*. Uncontrolled calcium sparks act as a dystrophic signal for mammalian skeletal muscle. *Nat Cell Biol* 2005;**7**:525–530.
6. Quinlan JG, Hahn HS, Wong BL, Lorenz JN, Wenisch AS, Levin LS. Evolution of the mdx mouse cardiomyopathy: physiological and morphological findings. *Neuromuscul Disord* 2004;**14**:491–496.
7. Alderton JM, Steinhardt RA. How calcium influx through calcium leak channels is responsible for the elevated levels of calcium-dependent proteolysis in dystrophic myotubes. *Trends Cardiovasc Med* 2000;**10**:268–272.
8. Guharay F, Sachs F. Stretch-activated single ion channel currents in tissue-cultured embryonic chick skeletal muscle. *J Physiol* 1984;**352**:685–701.
9. Tutdibi O, Brinkmeier H, Rüdel R, Fohr KJ. Increased calcium entry into dystrophin-deficient muscle fibres of mdx and adr-mdx mice is reduced by ion channel blockers. *J Physiol* 1999;**515**:859–868.
10. Petrof BJ, Shrager JB, Stedman HH, Kelly AM, Sweeney HL. Dystrophin protects the sarcolemma from stresses developed during muscle contraction. *Proc Natl Acad Sci USA* 1993;**90**:3710–3714.
11. Danialou G, Comtois AS, Dudley R, Karpati G, Vincent G, Des Rosiers C *et al*. Dystrophin-deficient cardiomyocytes are abnormally vulnerable to mechanical stress-induced contractile failure and injury. *FASEB J* 2001;**15**:1655–1657.
12. Yue Y, Skimming JW, Liu M, Strawn T, Duan D. Full-length dystrophin expression in half of the heart cells ameliorates β-isoproterenol-induced cardiomyopathy in mdx mice. *Hum Mol Genet* 2004;**13**:1669–1675.
13. Tidball JG, Albrecht DE, Lokensgard BE, Spencer MJ. Apoptosis precedes necrosis of dystrophin-deficient muscle. *J Cell Sci* 1995;**108**:2197–2204.
14. Mikhailov VM, Komarov SA, Nilova VK, Shtein GI, Baranov VS. Ultrastructural and morphometrical analysis of apoptosis stages in cardiomyocytes of mdx mice. *Tsitologiia* 2001;**43**:729–737.

15. Yasuda S, Townsend D, Michele DE, Favre EG, Day SM, Metzger JM. Dystrophic heart failure blocked by membrane sealant poloxamer. *Nature* 2005;**436**:1025–1029.
16. Williams IA, Allen DG. Intracellular calcium handling in ventricular myocytes from mdx mice. *Am J Physiol Heart Circ Physiol* 2007;**292**: H846–H855.
17. Jung C, Niggli E, Shirokova N. Amplification of cellular damage by Ca^{2+} signaling and ROS generating pathways in dystrophic cardiomyopathy. *Biophys J* 2007;**92**:255a.
18. Szentesi P, Pignier C, Egger M, Kranias EG, Niggli E. Sarcoplasmic reticulum Ca^{2+} refilling controls recovery from Ca^{2+}-induced Ca^{2+} release refractoriness in heart muscle. *Circ Res* 2004;**95**:807–813.
19. Wolska BM, Solaro RJ. Method for isolation of adult mouse cardiac myocytes for studies of contraction and microfluorimetry. *Am J Physiol* 1996;**271**:H1250–H1255.
20. Isaeva EV, Shirokova N. Metabolic regulation of Ca^{2+} release in permeabilized mammalian skeletal muscle fibres. *J Physiol* 2003;**547**: 453–462.
21. Zorov DB, Filburn CR, Klotz LO, Zweier JL, Sollott SJ. Reactive oxygen species (ROS)-induced ROS release: a new phenomenon accompanying induction of the mitochondrial permeability transition in cardiac myocytes. *J Exp Med* 2000;**192**:1001–1014.
22. Lindegger N, Niggli E. Paradoxical SR Ca^{2+} release in guinea-pig cardiac myocytes after β-adrenergic stimulation revealed by two-photon photolysis of caged Ca^{2+}. *J Physiol* 2005;**565**:801–813.
23. Lipp P, Niggli E. Ratiometric confocal Ca^{2+}-measurements with visible wavelength indicators in isolated cardiac myocytes. *Cell Calcium* 1993; **14**:359–372.
24. Shkryl VM, Shirokova N. Transfer and tunneling of Ca^{2+} from sarcoplasmic reticulum to mitochondria in skeletal muscle. *J Biol Chem* 2006;**281**: 1547–1554.
25. Menke A, Jockusch H. Extent of shock-induced membrane leakage in human and mouse myotubes depends on dystrophin. *J Cell Sci* 1995; **108**:727–733.
26. Pimentel DR, Amin JK, Xiao L, Miller T, Viereck J, Oliver-Krasinski J *et al*. Reactive oxygen species mediate amplitude-dependent hypertrophic and apoptotic responses to mechanical stretch in cardiac myocytes. *Circ Res* 2001;**89**:453–460.
27. Williams IA, Allen DG. The role of reactive oxygen species in the hearts of dystrophin-deficient (mdx) mice. *Am J Physiol Heart Circ Physiol* 2007; **293**:H1969–H1977.
28. Reinehr R, Gorg B, Becker S, Qvartskhava N, Bidmon HJ, Selbach O *et al*. Hypoosmotic swelling and ammonia increase oxidative stress by NADPH oxidase in cultured astrocytes and vital brain slices. *Glia* 2007;**55**: 758–771.
29. Brookes PS, Yoon Y, Robotham JL, Anders MW, Sheu SS. Calcium, ATP, and ROS: a mitochondrial love-hate triangle. *Am J Physiol Cell Physiol* 2004; **287**:C817–C833.
30. Hüser J, Blatter LA. Fluctuations in mitochondrial membrane potential caused by repetitive gating of the permeability transition pore. *Biochem J* 1999;**343**:311–317.
31. Yano M, Okuda S, Oda T, Tokuhisa T, Tateishi H, Mochizuki M *et al*. Correction of defective interdomain interaction within ryanodine receptor by antioxidant is a new therapeutic strategy against heart failure. *Circulation* 2005;**112**:3633–3643.
32. Yoshikawa Y, Hagihara H, Ohga Y, Nakajima-Takenaka C, Murata KY, Taniguchi S *et al*. Calpain inhibitor-1 protects the rat heart from ischemia–reperfusion injury: analysis by mechanical work and energetics. *Am J Physiol Heart Circ Physiol* 2005;**288**:H1690–H1698.
33. Davidson SM, Duchen MR. Calcium microdomains and oxidative stress. *Cell Calcium* 2006;**40**:561–574.
34. Payne TR, Oshima H, Sakai T, Ling Y, Gharaibeh B, Cummins J *et al*. Regeneration of dystrophin-expressing myocytes in the mdx heart by skeletal muscle stem cells. *Gene Ther* 2005;**12**:1264–1274.
35. Yue Y, Li Z, Harper SQ, Davisson RL, Chamberlain JS, Duan D. Microdystrophin gene therapy of cardiomyopathy restores dystrophin–glycoprotein complex and improves sarcolemma integrity in the mdx mouse heart. *Circulation* 2003;**108**:1626–1632.
36. Perkins KJ, Davies KE. The role of utrophin in the potential therapy of Duchenne muscular dystrophy. *Neuromuscul Disord* 2002;**12**: S78–S89.
37. Deconinck AE, Rafael JA, Skinner JA, Brown SC, Potter AC, Metzinger L *et al*. Utrophin–dystrophin-deficient mice as a model for Duchenne muscular dystrophy. *Cell* 1997;**90**:717–727.
38. Janssen PM, Hiranandani N, Mays TA, Rafael-Fortney JA. Utrophin deficiency worsens cardiac contractile dysfunction present in dystrophin-deficient mdx mice. *Am J Physiol Heart Circ Physiol* 2005;**289**:H2373–H2378.